International Research Journal of Natural and Applied Sciences
ISSN: (2349-4077)
Impact Factor- 5.46, Volume 4, Issue 12, December 2017
Website- www.aarf.asia, **Email** : editor@aarf.asia , editoraarf@gmail.com

PETROLOGY AND GEOCHEMISTRY OF ULTRAMAFIC XENOLITHS CUMULATS RELATED TO SEGUELA DIAMANDIFEOUS KIMBERLITE AND LAMPROITE (CENTRAL-WESTERN OF CÔTE D'IVOIRE).

M.E. Allialy[1]., S.C. Djro[1]; N. Houssou[1].,. A.N. Kouamelan[1]; J. Batumike[2]; Y. Coulibaly[1]; A. Gnanzou[1]; T. Boya[1]; O. Gbelé[3].
1. UFR-STRM, Université de Cocody Abidjan, Côte d'Ivoire 22 B.P. 582 Abidjan 22

2. GEMOC ARC National Key Centre, Department of Earth and Planetary Sciences, Macquarie University, NSW 2109, Sydney, Australia
3. STRMi, INPHB, Yamoussoukro,

ABSTRACT

The Seguela kimbelites located 30 km North of Seguela city in the central-western part of Ivory Coast are chracterised by the presence of a lot of olivine pyroxenite xenoliths that are characteristic of the lithospheric mantle. The study of these xenoliths provides an opportunity of understanding the lithospheric mantle underneath the region. These xenoliths are formed by olivine (forsterite; Fo_{90}), enstatite, phlogopite, amphibole, chromites and Cr-spinels. Enstatites have relatively high Mg# ($Mg/(Mg+Fe^{2+})$) >0.8. The olivine pyroxenite xenoliths have Mg# higher than the host kimberlite, and their high Cr (>3000 ppm), Ni ((>1000 ppm), Co, Cu, V, and Zn contents are indicative of affinity with alkaline ultramafic rocks.

Compared with kimberlites, these olivine pyroxenite xenoliths show high enrichment in HFSE, LILE, REE. Their low La/Yb (<14) ratios, and Ba (<150 ppm), Rb (<50 ppm) and Nb (<6 ppm) contents indicate high degree of partial melting. Zr/Hf (39) and Nb/Ta (14) ratios support their lithospheric mantle origin. The age of these olivine pyroxenite xenoliths as derived from zircon is Paleoproterozoic. The geochemical signatures observed on these olivine pyroxenite are different from those of continental basalts. This indicate that the arc magmatism in the region derived from ancient subduction process in that affected the *composition of the lithospheric mantle modification and lead to the continental tholeiitic arc signatures observed on olivine pyroxenite xenoliths from Côte d'Ivoire.*

Keywords: Xenoliths cumulats, geochemistry; cretaceous kimberlites, petrogenesis, Côte d'Ivoire.

Introdction

West African craton kimberlites and related rocks [1] include concentrations of kimberlites in South-eastern Guinea, in eastern Sierra, in western Liberia and in Côte d'Ivoire. Diamond occurrences were discovered using traditional prospecting and indicator minerals based on the Diamondiferous Mantle Root'' (DMR) concept. The diamondiferous mantle root model (DMR Model) is well described by [2]), [3], [4] The mantle-derived indicator mineral suite of the Man craton kimberlites and related rocks is well represented by ilmenite, chromite, olivine, amphibole, mica and orthopyroxene. These indicator minerals have previously been studied by various researchers (e.g., [2], [5]). Discovery of a diamond-bearing kimberlite diatrem in Seguela ([5], [6], [7], [8],[9],[11]) shown that abundant olivine, pyroxene, amphibole, mica, megacrysts ; chromite, Cr-spinels, Mg-ilmenite, and lack of garnet in ultramafic xenoliths cumulates. This paper presents a summary and preliminary assessment of the geology, petrography and mineral chemistry of the Seguela ultramafic xenoliths cumulates related to kimberlite and lamproite.

1. GEOLOGICAL SETTING

Seguela diamond-bearing kimbelite field is located in the central-western part of Ivory Coast, 30 km North of Seguela city (Fig. 2). In this region diamonds are found disseminated into eluvia, colluvia and alluvia with an average of 0.3 ct and the source for the diamonds is considered to be the two main kimberlitic dykes of Bobi and Toubabouko. Two companies (Waston & SODEMI) have been active in mining activities in the places with higher diamond concentration in the filed from Bobi to Toubabouko. In the present days, there is no more industrial activity and only individual diggers are working in the area. The dykes, trending N170°E, crosscut the granitic plutons and amphibolites of the Palaeoproterozoic Birimian formations of the West-African Craton. The Seguela granite is dated at 2091 Ma ([7], [4]). The dyke of Bobi is 2.5 km long and 25 to 50 cm wide. Length of the dyke of Toubabouko reaches 4.5 km with 80 cm to 1 m thickness. In the northern part of this dyke, a particularly enriched zone was recently discovered forming a 80-m-diameter large area and 30-m-deep pit

(N 8°15’ 22’’, W 6°37’ 57’’) (Figs.1, 2). The age of the Seguela kimberlites is not yet constrained but they are supposed to be Cretaceous, like other occurrences inside West Africa Craton.

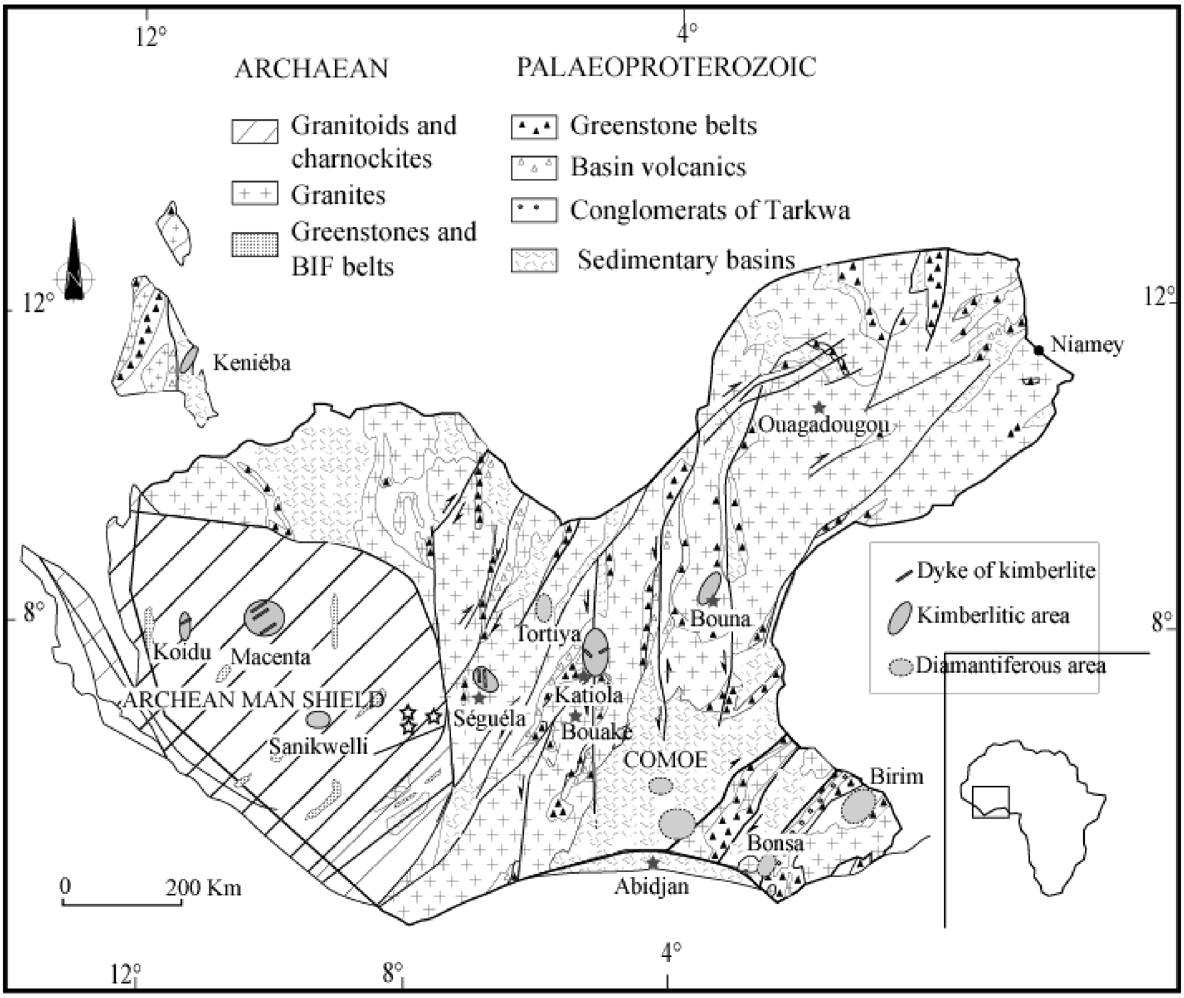

Figure 1 Fig.1. Simplified geological map showing tectono-stratigraphic provinces of archeans and paleoproterozoic formations of the Man Shield (West Africa craton). Modified from [1].

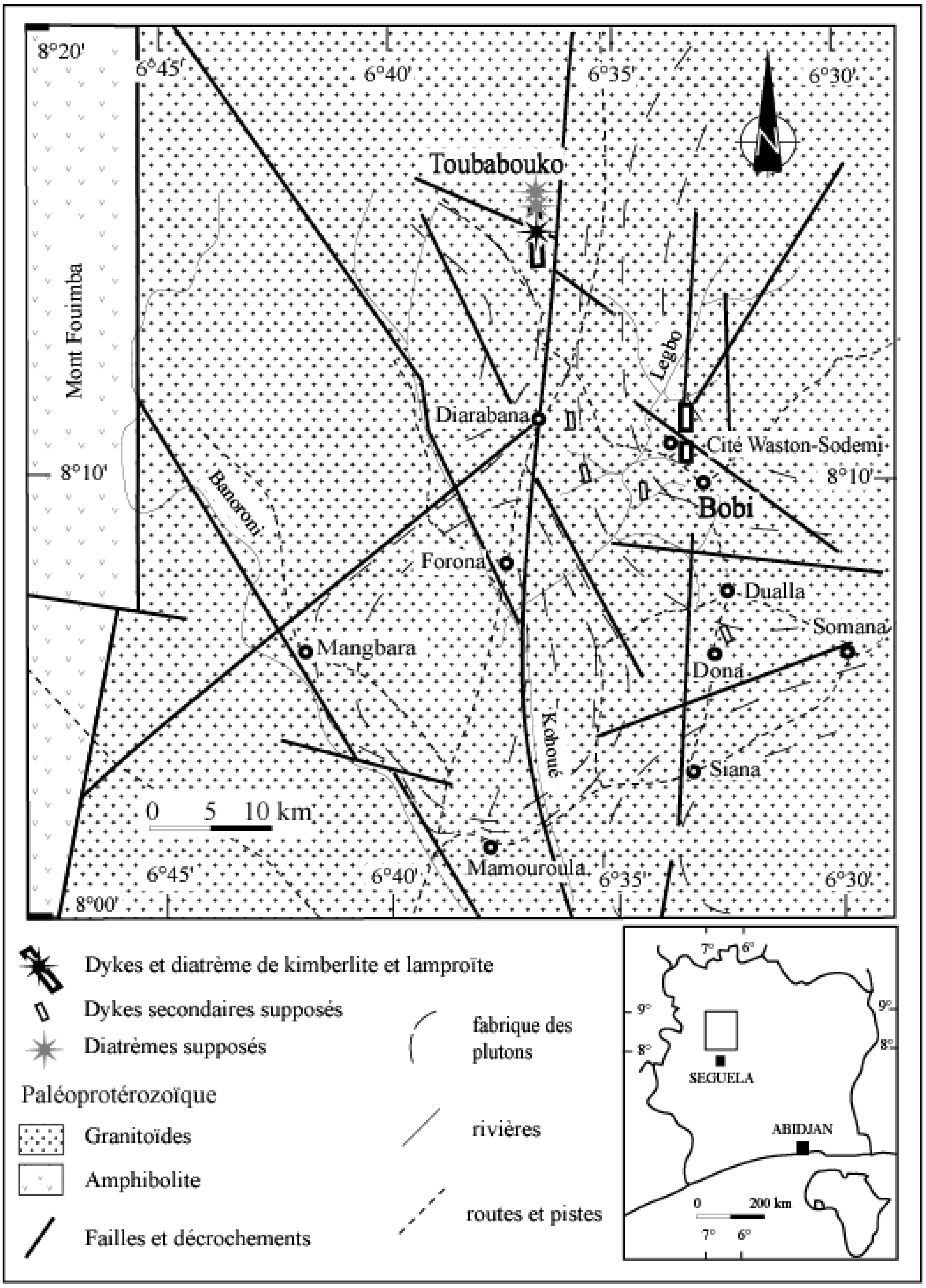

Figure 2 : Geological map of Seguela area in Côte d'Ivoire [7].

2. METHODOLOGY

The geochemical data were realized within the analytical laboratory of the CRPG (Nancy, France). Major oxide analyses were obtained using emission spectroscopy on

ICP-AES whereas trace-element geochemistry were determined by mass spectroscopy on ICP-MS. Results for both major and trace elements are given in Table 1. Samples were chipped and cleaned in acid before being crushed and powdered. Powders were mixed by coning several times to ensure homogeneity. 300 mg of the powdered sample were considered for determination of loss on ignition by living the samples in a muffle furnace at 1000°C for 12 hours. For preparation of glass fusion discs, sample was mixed with lithium tetraborate (LiBO3) and the mixture was heated in a furnace to 1050°C and cast in carbon dies to form the discs. Major elements, together with V, Cr, Ni, Zn, Ga, Rb, Sr, Y, Zr, Nb, Ba, La, Ce, Pb, and Th were analysed on the prepared discs by X-Ray fluorescence (XFR) spectrometer at the Centre de Recherche Pétrographique et Géochimique de Nancy (France) using spectrometer ICP-AES Jobin Yvon JY70 for major element(Si, Al, Fe total, Mn, Mg, Ca, Na, K, P, Ti).The comparative database KIMDAT was extracted from the primitive alkaline rock database of [3], [9], [10] for comparison between our data and other occurrences. This database contains ≈ 260 chemical analyses of kimberlites and ultrabasic rocks, including olivine lamproites and aillikites (central-complex kimberlite of [9, 11]; believed to originate in the deeper mantle (e.g [12], [10]). KIMDAT was screened to eliminate effect of fractionation, contamination and alteration on the samples (see [9]) because kimberlites and olivine lamproites are susceptible to deuteritic alteration, weathering, and xenolith contamination.

3. PETROLOGY

The petrographic textures show variable grain sizes and modal variations throughout the xenolith cumulate. Original xenoliths mineralogy has been recognised from the relic coarse grained textures: cumulate olivine pyroxenites. The cumulates show distinctive textures with intercumulus and cumulus phases. The cumulus phases are olivine and orthopyroxene whilst the intercumulus phases are amphibole and/ or mica.

3.1. Olivine

The olivine composition in xenoliths is forsteritic, ranging from Fo75 to Fo 8. This is significantly more Fe-rich than normal mantle values (-Fo88.92). In some xenoliths, the olivine has clearly been partially replaced by secondary phlogopite mica, which cuts large optically continuous grains. Olivine in the xenoliths shows one population with cores and larger grains. Olivine in the cumulates is typically with more magnesian olivine has Fo>88 (Table 1).

3.2. Pyroxene

The orthopyroxenes found in most of the xenoliths are enstatitic, (Wo %<0; Fs%<15; En% >80). Much of the enstatite in xenolith cumulat T025 and TS4 contains significant MgO (32 wt%). however most pyroxene has Cr_20_3<0.2. They contain slight Na in excess of Al consistent with a minor acmite component indicating weakly peralkaline conditions. However, calculated acmite contents for the xenolith orthopyroxenes are low (Table 1).

The *Mg* is variable but mostly falls in the range Mg84 to.90. The orthopyroxenes in the majority of cumulates have Fe/Fe+Mg <0.1. Low Ti-pyroxenes in the xenolith overlap fields for more primitive kimberlite, lamproites and orangeites with notably lower Al and Ti (Table 2).

Table 1 : Geochemistry analysis of amphiboles megacrysts samples from ultramafic xenoliths cumulats

SEGUELA
OLIVINES
Xenoliths

	T-25							T-S04			
n° anal	34	41	42	43	52	59	64	15	20	35	36
SiO2	40,10	39,94	39,94	40,17	40,19	41,07	40,54	40,89	41,74	41,23	41,82
TiO2	0,00	0,00	0,00	0,00	0,03	0,00	0,00	0,05	0,00	0,01	0,03
Al2O3	0,00	0,01	0,00	0,00	0,00	0,00	0,03	0,00	0,01	0,00	0,04
FeO	11,81	11,04	11,31	10,00	10,82	10,40	11,68	13,77	13,91	13,72	14,37
MnO	0,38	0,13	0,24	0,26	0,29	0,28	0,16	0,38	0,21	0,12	0,28
MgO	48,45	48,35	48,25	49,94	48,92	48,15	48,30	45,24	46,01	46,11	46,17
CaO	0,00	0,00	0,00	0,00	0,00	0,00	0,00	0,00	0,00	0,00	0,00
NiO	0,00	0,00	0,00	0,00	0,00	0,00	0,00	0,00	0,00	0,00	0,00
Total	100,74	99,47	99,74	100,38	100,26	99,90	100,71	100,32	101,87	101,19	102,71
Formule structurale											
Si	0,99	0,99	0,99	0,98	0,99	1,01	0,99	1,02	1,02	1,01	1,01
Ti	0,00	0,00	0,00	0,00	0,00	0,00	0,00	0,00	0,00	0,00	0,00
Al	0,00	0,00	0,00	0,00	0,00	0,00	0,00	0,00	0,00	0,00	0,00
Fe2+	0,24	0,23	0,23	0,20	0,22	0,21	0,24	0,29	0,28	0,28	0,29
Mn	0,01	0,00	0,01	0,01	0,01	0,01	0,00	0,01	0,00	0,00	0,01
Mg	1,78	1,79	1,78	1,82	1,79	1,76	1,77	1,67	1,67	1,69	1,67
Ca	0,00	0,00	0,00	0,00	0,00	0,00	0,00	0,00	0,00	0,00	0,00
NI	0,00	0,00	0,00	0,00	0,00	0,00	0,00	0,00	0,00	0,00	0,00
Total	3,01	3,01	3,01	3,02	3,01	2,99	3,00	2,98	2,98	2,99	2,98
% Forstérite	87,63	88,53	88,15	89,66	88,70	88,93	87,91	85,08	85,32	85,59	84,89
% Fayalite	12,37	11,47	11,85	10,34	11,30	11,07	12,09	14,92	14,68	14,41	15,11
Mg#	0,88	0,89	0,88	0,90	0,89	0,89	0,88	0,85	0,85	0,86	0,85

Table 2: Geochemistry analysis of orthopyroxenes samples from Seguela xenoliths cumulats

Seguela Orthopyroxenes								
n°ech	T 025			T-S04				
n° anal	106	107	108	16	22	27	29	34
SiO2	55,52	54,75	55,78	58,49	57,64	57,93	56,70	57,89
TiO2	0,00	0,09	0,00	0,03	0,08	0,00	0,01	0,12
Al2O3	1,90	1,71	1,83	0,58	1,46	1,07	1,52	1,08
FeOt (enter)	9,99	9,64	9,48	10,40	10,40	9,87	9,71	10,36
Fe2O3 (calc.)	2,04	3,34	1,75	0,00	0,00	0,00	0,00	0,00
FeO (calc.)	8,16	6,64	7,91	10,40	10,40	9,87	9,71	10,36
Cr2O3	0,23	0,02	0,03	0,07	0,16	0,09	0,13	0,02
MnO	0,21	0,29	0,29	0,25	0,26	0,32	0,28	0,34
MgO	32,35	32,73	32,68	32,36	31,45	32,18	31,72	31,99
CaO	0,24	0,21	0,15	0,07	0,20	0,20	0,17	0,14
Na2O	0,01	0,00	0,00	0,00	0,00	0,04	0,03	0,00
K2O	0,00	0,01	0,02	0,00	0,00	0,02	0,00	0,00
Total (FeOt)	100,46	99,45	100,27	102,25	101,65	101,71	100,27	101,94
T Fe calc	100,66	99,79	100,45	102,25	101,65	101,71	100,27	101,94
Formule structurale								
Si	1,93	1,92	1,94	2,00	1,99	1,99	1,98	1,99
Ti	0,00	0,00	0,00	0,00	0,00	0,00	0,00	0,00
Al IV	0,07	0,07	0,06	0,00	0,01	0,01	0,02	0,01
Al VI	0,01	0,00	0,01	0,02	0,04	0,03	0,04	0,03
Fe3+	0,05	0,09	0,05	0,00	0,00	0,00	0,00	0,00
Fe2+	0,24	0,19	0,23	0,30	0,30	0,28	0,28	0,30
Cr	0,01	0,00	0,00	0,00	0,00	0,00	0,00	0,00
Mn	0,01	0,01	0,01	0,01	0,01	0,01	0,01	0,01
Mg	1,68	1,71	1,69	1,65	1,62	1,65	1,65	1,64
Ca	0,01	0,01	0,01	0,00	0,01	0,01	0,01	0,01
Na	0,00	0,00	0,00	0,00	0,00	0,00	0,00	0,00
K	0,00	0,00	0,00	0,00	0,00	0,00	0,00	0,00
Total	4,00	4,00	4,00	3,99	3,98	3,99	3,99	3,99
Xfe=Fe2/Fe2+Mg	0,12	0,10	0,12	0,15	0,16	0,15	0,15	0,15
Mg %	84,58	85,11	85,38	84,29	83,70	84,60	84,70	83,97
Fe t + Mn %	14,97	14,50	14,34	15,57	15,92	15,03	14,97	15,76
Ca %	0,45	0,39	0,29	0,14	0,38	0,37	0,33	0,27
En %	86,42	89,15	86,35	82,36	80,13	81,85	81,52	81,27
Fs %	12,54	10,59	12,16	15,22	15,24	14,54	14,41	15,25
Wo %	0,00	0,00	0,00	0,00	0,00	0,00	0,00	0,00
Ac %	0,00	0,00	0,00	0,00	0,00	0,00	0,00	0,00
Jd %	0,00	0,00	0,00	0,00	0,00	0,00	0,00	0,00
Ca-Tsch %	0,96	0,00	1,49	2,35	4,42	3,37	3,85	3,19
Ti-Tsch %	0,00	0,24	0,00	0,06	0,21	0,00	0,02	0,29
Es %	0,00	0,00	0,00	0,00	0,00	0,00	0,00	0,00
Ko%	0,08	0,02	0,00	0,01	0,01	0,23	0,21	0,00
Total	100,00	100,00	100,00	100,00	100,00	100,00	100,00	100,00

3.3. Amphibole-pargasite or hornblende-pargasite and tschermakite.

The amphibole megacrysts are often embayed or anhedral in shape and are slightly larger (up to 15 crn long) than the pyroxene megacrysts. The crystals are dark brown, or black in colour and some have small white zeolite inclusions (< 1 ram). Occasional concentric zones seen in thin section show no detectable chemical zonation and they have uniform compositions close to pargasite or hornblende-pargasite. Some contain trails of linked, spherical melt 'blobs' (-20 microns in diameter) of decompression melt and partly evacuated fluid inclusion trails. These trails are often parallel and many contain quench crystals of magnetite, ilmenite and chromite. Pargasitic amphibole is present in all xenoliths (e.g. cumulate T025, and TS4). The amphibole found in the cumulates, is essentially pargasitic hornblende, and is rather similar to the megacryst amphibole. The xenolith amphiboles are more primitive, and have Mg# =1; Na/ (Na + K) = 0.95. In cumulate T025 small areas of a second type of amphibole can be found as corroded relics; namely tschermakite. The crystals are TiO_2-poor (0.55 wt%) with negligible Chromium (< 0.44 wt% Cr_20_3; See Table 3).

3.4. Mica

Mica from xenoliths cumulats olivine pyroxenite have similar compositions to megacrysts phlogopite . Phlogopite with TiO_2 content varying from (0 -5%) and Cr_2O_3 (0 - 1.1%) different to primary and secondary phlogopite. Xenoliths cumulats phlogopites present affinity to type A phlogopites characterised by zonated yellow grains. Mg# varying from 0.87% to 0.9%, Cr_2O_3 (< 0.25%) and TiO_2 (< 2%). In comparison with phlogopites from Seguela kimberlites and lamproites have respectively TiO_2 (2.6 - 5.11%) ; Mg# (0.87 - 1%) and Cr_2O_3 (0.0 – 0.36%) content which show type B phlogopites affinity ([19]). The xenolith mica compositions are not distinct from the megacrysts and also lie inside the fields for micas from the mantle and more primitive kimberlites and orangeites (Table 4).

3.5. Chromite, Cr-spinels, Ilmenite and Magnetite

Chromites and Cr-spinels grains from xenoliths samples were located as a small inclusion in olivine nodules. The majority of Seguela chromites inclusions and Cr-spinels define a narrow compositional range, analogous to chromites and Cr-spinels from localities worldwide ([10, 17]). The Seguela Cr-Ti chromites are phenocrysts crystallized from TiO_2-rich xenoliths magmas derived from lithospheric mantle. They contain more than 0.8 wt % TiO_2. These chromites have average Cr_2O_3(30-45wt %) value and relatively constant TiO_2 (3.43 - 5.71 wt %).

Ilmenite is found in xenoliths as small irregular grain (crystals 20µm-30µm), as large (1- 5mm) ovoid nodules and as eutectic like intergrowths with enstatite. The eadges of the grains and nodules are typically rimmed by perovskite forme by reaction of ilmenite with the groundmass fluid reaction of the kimberlite. Sometimes ilmenite and magnetite are observed in olivine or phlogopite cleavage. Two variety of ilmenite (Mn-ilmenite and M-gilmenite) are distinguished in Seguela xenoliths. Mn-ilmenite Aboundance Mn-ilmenite are characterized by high TiO_2 (46-56 wt%), high MnO (4-19 wt%) and relatively low MgO (< 0.63wt%) contents.

Ti-Magnetite population is represented by small automorph crystals (50µm) observed in phlogopite or derived from olivine serpentinisation. Mg Ti-Magnetite are characterized by higher Fe^{3+}+ Ti (> 0.9) and Fe^{2+}/ Fe^{2+}+ Mg (> 0.8) ratios.

Table 3 : Geochemistry analysis of amphiboles megacrysts samples from ultramafic xenoliths cumulats

© **Associated Asia Research Foundation (AARF)**
A Monthly Double-Blind Peer Reviewed Refereed Open Access International e-Journal - Included in the International Serial Directories.

Amphiboles

Orthopyroxénite à olivine

	T025											
N° Analyse	38	39	44	48	55	58	95	97	98	100	102	105
SiO2	46.31	46.10	45.52	44.80	48.09	55.64	44.27	47.41	46.84	52.80	52.83	46.00
TiO2	0.41	0.28	0.31	0.38	0.50	0.06	0.84	0.46	0.74	0.27	0.26	0.48
Al2O3	9.78	10.87	10.64	11.26	8.58	1.66	11.33	8.26	8.98	5.15	3.58	9.70
Cr2O3	0.44	0.55	0.62	0.63	0.46	0.03	0.30	0.46	0.45	0.09	0.23	0.56
FeO t	5.38	5.29	5.07	5.67	4.33	2.64	6.43	3.98	4.93	4.21	6.64	5.65
MnO	0.09	0.10	0.13	0.15	0.13	0.23	0.10	0.00	0.08	0.23	0.09	0.23
MgO	20.01	19.70	20.77	18.78	20.36	23.58	18.81	23.30	20.86	22.39	18.73	19.65
CaO	12.20	11.80	10.58	11.39	12.15	12.18	11.86	9.65	10.96	11.65	12.55	11.86
Na2O	2.50	2.63	1.88	2.44	1.78	0.33	2.59	1.46	1.62	1.16	0.58	2.25
K2O	0.14	0.16	0.56	0.21	0.23	0.04	0.43	1.87	1.14	0.08	0.29	0.52
Fe2O3 calc	5.98	5.87	5.63	6.30	4.81	2.94	7.14	4.42	5.48	4.67	1.43	6.28
FeO calc	0.00	0.00	0.00	0.00	0.00	0.00	0.00	0.00	0.00	0.00	5.36	0.00
Total	97.25	97.48	96.08	95.70	96.60	96.39	96.95	96.86	96.60	98.02	95.78	96.91
Formule structurale												
Site tetraédrique												
Si	6.47	6.41	6.28	6.34	6.71	7.60	6.24	6.42	6.49	7.13	7.54	6.46
AlIV	1.53	1.59	1.72	1.66	1.29	0.27	1.76	1.32	1.47	0.82	0.46	1.54
Ti	0.00	0.00	0.00	0.00	0.00	0.01	0.00	0.06	0.04	0.04	0.00	0.00
Total IV	8.00	8.00	8.00	8.00	8.00	7.87	8.00	7.80	8.00	7.98	8.00	8.00
Site octaédrique												
AlVI	0.09	0.19	0.02	0.22	0.12	0.00	0.13	0.00	0.00	0.00	0.15	0.07
Ti	0.06	0.04	0.04	0.05	0.07	0.00	0.12	0.00	0.06	0.00	0.04	0.07
Cr	0.05	0.06	0.07	0.07	0.05	0.00	0.03	0.05	0.05	0.01	0.03	0.06
Fe3	0.01	0.01	0.01	0.02	0.02	0.03	0.01	0.00	0.01	0.03	0.01	0.03
Fe2	0.00	0.00	0.00	0.00	0.00	0.00	0.00	0.00	0.00	0.00	0.64	0.00
Mn	0.01	0.01	0.01	0.02	0.02	0.03	0.01	0.00	0.01	0.03	0.01	0.03
Mg	4.17	4.08	4.27	3.96	4.24	4.80	3.95	4.70	4.31	4.51	3.99	4.11
Ca	0.62	0.60	0.57	0.65	0.49	0.15	0.75	0.25	0.56	0.43	0.14	0.64
Total VI	5.00	5.00	5.00	5.00	5.00	5.00	5.00	5.00	5.00	5.00	5.00	5.00
Site B												
Mg	0.00	0.00	0.00	0.00	0.00	0.00	0.00	0.00	0.00	0.00	0.00	0.00
Fe2	0.00	0.00	0.00	0.00	0.00	0.00	0.00	0.00	0.00	0.00	0.00	0.00
Mn	0.00	0.00	0.00	0.00	0.00	0.00	0.00	0.00	0.00	0.00	0.00	0.00
Ca	1.83	1.76	1.57	1.73	1.82	1.78	1.79	1.40	1.63	1.68	1.92	1.79
Na	0.17	0.24	0.43	0.27	0.18	0.09	0.21	0.38	0.37	0.30	0.08	0.21
total B	2.00	2.00	2.00	2.00	2.00	1.87	2.00	1.78	2.00	1.99	2.00	2.00
Site A												
Na	0.51	0.47	0.07	0.40	0.30	0.00	0.50	0.00	0.06	0.00	0.08	0.40
K	0.02	0.03	0.10	0.04	0.04	0.01	0.08	0.32	0.20	0.01	0.05	0.09
Total A(Na+K)	0.53	0.50	0.17	0.44	0.34	0.01	0.58	0.32	0.27	0.01	0.13	0.49
XMg = Mg/(Mg+Fe2	1.00	1.00	1.00	1.00	1.00	1.00	1.00	1.00	1.00	1.00	0.86	1.00

Table 4: Geochemistry analysis of phlogopites samples from ultramafic xenoliths cumulats

SEGUELA Phlogopites									
N° Ech	T-S4 Xenoliths					T 025 Xenoliths			
N° Anal	32	41	42	43	Moyenne	46	49	56	103
SiO2	40,06	39,01	39,49	39,30	39,53	39,87	40,47	40,18	39,30
Al2O3	11,09	10,54	10,78	10,61	10,68	12,41	13,59	12,94	14,05
TiO2	5,22	5,52	5,50	5,09	5,28	0,28	0,65	0,57	0,67
FeO	4,25	4,54	4,19	4,31	4,34	2,49	3,05	3,08	3,74
MgO	22,13	22,81	23,17	23,24	22,81	29,00	26,48	25,72	26,35
CaO	0,27	0,00	0,00	0,00	0,06	0,28	0,21	0,36	0,24
MnO	0,00	0,00	0,02	0,00	0,01	0,00	0,00	0,00	0,00
Cr2O3	0,53	0,19	0,20	0,30	0,36	0,00	0,00	0,00	0,01
K2O	9,53	10,04	9,95	10,01	9,88	8,32	9,82	9,58	9,75
Na2O	0,09	0,06	0,08	0,05	0,05	0,20	0,31	0,26	0,21
Total	93,16	92,71	93,37	92,91	93,00	92,86	94,58	92,69	94,31
Formule structurale									
Si	3,18	3,13	3,14	3,14	3,15	3,12	3,14	3,18	3,07
Al	1,04	1,00	1,01	1,00	1,00	1,15	1,24	1,21	1,29
Ti	0,31	0,33	0,33	0,31	0,32	0,02	0,04	0,03	0,04
Fe	0,28	0,31	0,28	0,29	0,29	0,16	0,20	0,20	0,24
Mg	2,62	2,73	2,74	2,77	2,71	3,39	3,06	3,03	3,07
Ca	0,02	0,00	0,00	0,00	0,01	0,02	0,02	0,03	0,02
Mn	0,00	0,00	0,00	0,00	0,00	0,00	0,00	0,00	0,00
Cr	0,03	0,01	0,01	0,02	0,02	0,00	0,00	0,00	0,00
K	0,97	1,03	1,01	1,02	1,01	0,83	0,97	0,97	0,97
Na	0,01	0,01	0,01	0,01	0,01	0,03	0,05	0,04	0,03
Total	8,46	8,55	8,53	8,56	8,52	8,72	8,71	8,69	8,75
XFe	0,10	0,10	0,09	0,09	0,10	0,05	0,06	0,06	0,07
(*Al'*)	0,82	0,87	0,86	0,86	0,85	0,88	0,86	0,82	0,93
AlIV	0,82	0,87	0,86	0,86	0,85	0,88	0,86	0,82	0,93
AlVI	0,22	0,13	0,15	0,14	0,16	0,27	0,38	0,38	0,37
Mg#	90,27	89,95	90,77	90,58	90,35	95,41	93,93	93,71	92,62

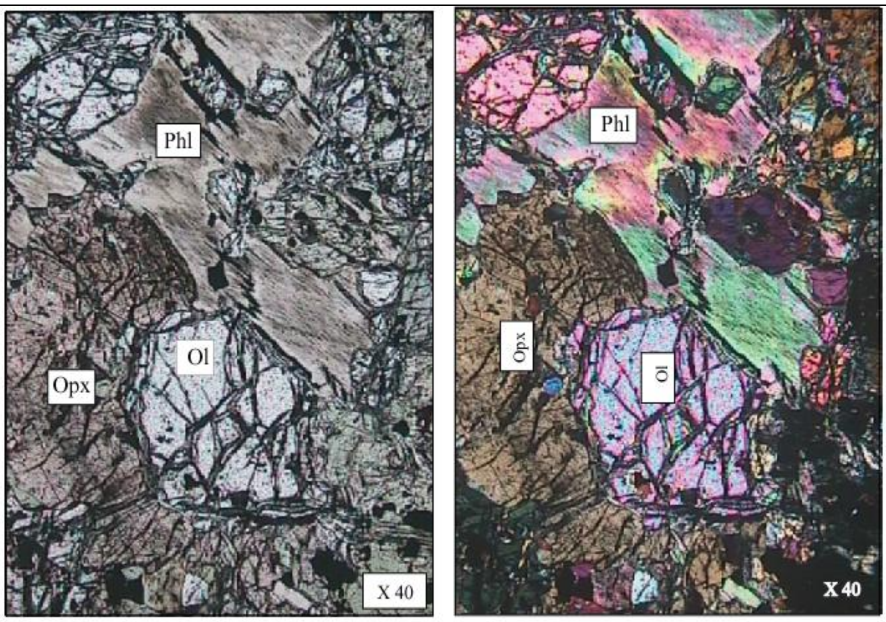

Figure 3 :Microphotography of Seguela Kimberlites xenolits cumulates (T025)

© **Associated Asia Research Foundation (AARF)**
A Monthly Double-Blind Peer Reviewed Refereed Open Access International e-Journal - Included in the International Serial Directories.

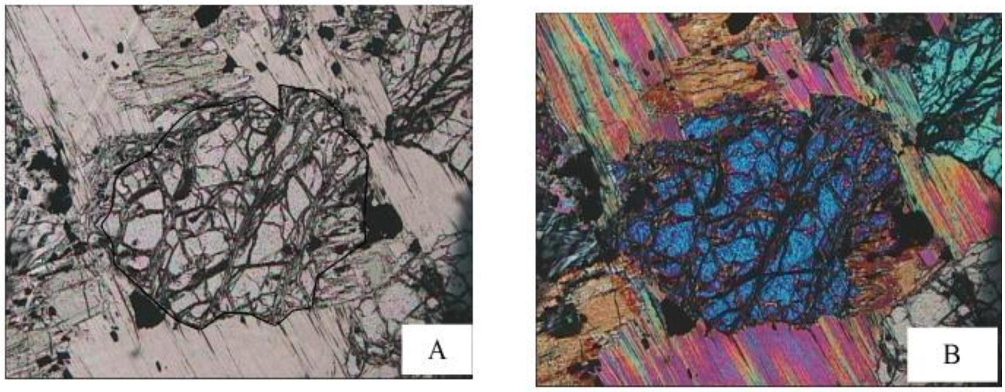

Figure 4 : Microphotography A and B of olivine, phlogopite megacryts and oxides

from Seguela kimberlites xenoliths cumulates

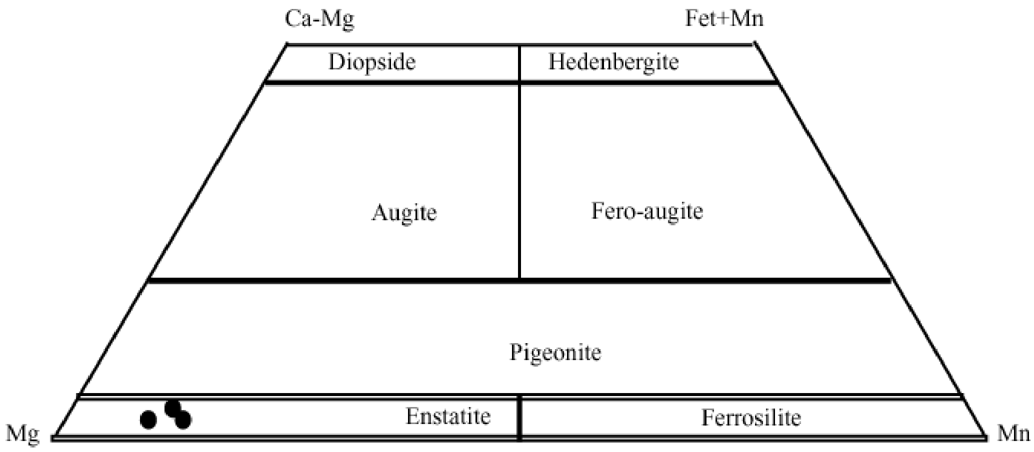

Figure 5: Pyroxene megacrysts samples plotted on a Ca-Mg-Fet +Mn- Mn-Mg diagram

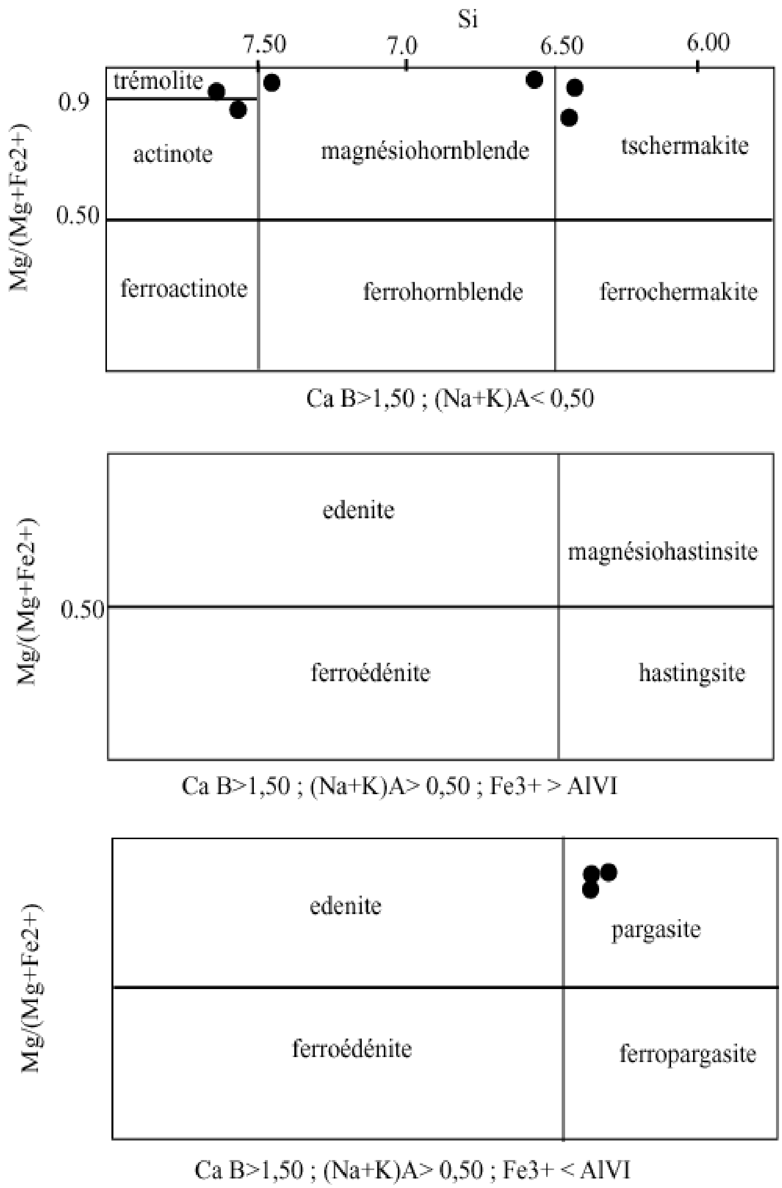

Figure 6 : Amphiboles megacrysts samples plotted on a Mg/(Mg+Fe^{2+}) vs Ca ;(Na+K); Fe^{3+} diagram [13].

4. GEOCHEMISTRY

4.1. Major elements geochemistry

Samples T-25 et T-S4 analysis are given in table1. Xenoliths cumulats SiO_2 ratios vary to 35% at 51%. These samples presents high contents in MgO (29 - 40 %). This richness in magnesium is related to Mg-olivines presence (Fo88 - 91). Ratios in K_2O (K_2O < 0,48%) and Na_2O (Na_2O < 0,54%) are generally lower. Xenoliths are also poor in titane (TiO_2 < 0,32%). Very high Contents in Cr (3100 ppm) and Ni (994 - 1079 ppm) are presented in Table 5 ;6).

4.2. Trace and REE elements geochemistry

Traces elements data including rare earth elements (REE) and high-field-strength elements (HFSE) are listed in Table 5 and 6.

Traces elements values are generally higher than dosability limits. Toubabouko xenoliths cumulates are poor in REE. In comparison with kimberlite and lamproite from Seguela xenoliths cumulates (T025 and TS4) are enriched in Cs, Ba, Rb, U et Sm on the other hand poor in Th, Nb, La, Sr, Zr, Hf et Ti (HFSE). Figures (X and Y). We notice that a slight enrichment in TR from Terbium (Tb/Lu=1.93 - 2.26) and negative anomaly in Nb and Ta, (Nb/La_n= 0.25 - 0.97 ; Nb/Th_n = 2.68- 7.43) Th, Zr-Hf, et Ti. Sample T-S4 is enriched in Ta (anomalie positive). The HFSE (Zr, Hf, Ti) are slightly poor (Figures 7 and 8). Negative anomalie origin in Ta-Nb associated with Ti and Zr from magmatic arc is explained by :

- Nb and Ta are fractionated and metasomatosed upper mantle source [4].
- Anomalie in HSFE derived from reaction whithin basaltic and peridotitic liquidus

from primitive mantle (Kelemen et al, 1993). The ratios La/Yb (8.69 – 14) and Nb/Th (2.68 - 7.43) are higher than others orthopyroxenites cumulates from Ivory Coast [7]. The Seguela xenolith have steep REE patterns which are similar to average kimberlites and related rocks [4]. Comparative element abundance plots normalized against primitive mantle values (Fig.) show marked large-ion lithophile element (LILE) and LREE enrichments (> 100 times primitive mantle abundance) with pronounced positive Rb, Nd, and Sm anomalies, and negative Sr, P, Hf, Zr anomalies. These are all features previously documented for kimberlites and related rocks [3], [4], [8].

Table 5 : Geochemistry analysis of ultramafic xenoliths cumulats from Seguela

SEGUELA					
Rocks total analysis	Olivine Lamproite Bobi	Kimberlite Toubabouko	Kimberlite micaceous Toubabouko	**Xenoliths cumulats**	
	K-11	K-12	K-3B2	**T025**	**T- S4**
SiO2	36,95	49,75	55,60	42,30	41,84
Al2O3	7,11	4,35	1,61	4,59	4,62
Fe2O3	10,25	6,84	6,12	14,90	15,04
MnO	0,14	0,11	0,05	0,20	0,19

MgO	20,27	21,28	26,43	29,52	31,22
CaO	8,10	5,48	1,31	3,65	3,73
Na2O	0,72	0,24	0,10	0,54	0,72
K2O	1,11	0,20	0,73	1,13	0,48
TiO2	3,98	2,61	1,52	0,32	0,33
P2O5	1,36	1,16	0,64	0,09	0,09
Pf	9,45	8,05	6,00	2,78	1,91
Total	99,46	99,93	100,02	100,02	100,17
Mg#	66,42	75,68	81,20	66,46	67,49

Table 6 : Comparison between xenoliths, kimberlite lamproites and worldwides rocks minor and REE [8].

Rocks samples	K-11 Lamproite	K-12 Kimberlite	K-3B2 Kimberlite	T-25 Xenolith	T- S4 Xenolith	Z1-2-1 Kimberlite	Z1-2-2 Kimberlite	Mura 83 Kimberlite
Ni/Cr	0,51	0,88	2,55	0,34	0,31	0,89	1,20	1,08
La/Nb	1,21	1,30	0,06	4,06	1,04	0,98	0,73	1,06
La/Ba	0,88	0,39	0,14	0,02	0,02	0,05	0,04	0,21
(La/Yb)n	309,09	323,35	119,64	14,00	8,69	101,67	75,83	125,00
Th/Yb	22,45	20,10	15,29	1,28	1,13	4,44	1,88	14,17
Ta/Yb	14,82	14,48	7,69	0,24	2,42	5,65	6,25	9,17
Ce/Y	20,30	12,90	9,71	6,00	7,52	8,30	8,60	22,00
Ti/Y	768,47	1851,16	616,68	320,00	171,94	500,48	428,37	536,36
Ta/Hf	0,79	0,74	0,54	0,13	1,87	1,53	1,07	1,96
Th/La	0,07	0,06	0,13	0,09	0,13	0,04	0,02	0,11
Ti/K	1,79	6,53	1,04	0,14	0,34	0,38	0,28	
Ba/Sr	0,77	0,13	1,14	1,11	0,75	1,17	2,43	1,29
Ce/Pb	30,93	71,47	8,51	15,18	13,71			13,07
Ba/Nb	3,31	0,59	5,32	80,00	19,54	7,48	15,56	7,80
Zr/Hf	45,07	46,09	37,59	39,00	35,53	44,00	43,21	32,86

Zr/Nb	3,31	3,61	4,10	21,08	5,48	1,57	2,42	1,30
Th/Pb	1,28	2,39	0,47	0,62	0,71			1,11
La/Lu	1942,86	2564,36	1123,94	86,44	54,40	610,00	520,00	937,50
P2O5/Ce *	22,78	24,12	34,97	52,94	56,60	86,68	68,86	0,00
Nb/Zr	0,30	0,28	0,24	0,05	0,18	0,64	0,41	0,77
Nb/U*	103,68	68,86	51,72	6,61	29,00	101,82	416,67	45,48
Ba/Rb	25,80	26,12	78,97	4,87	7,73	7,19	16,52	15,07

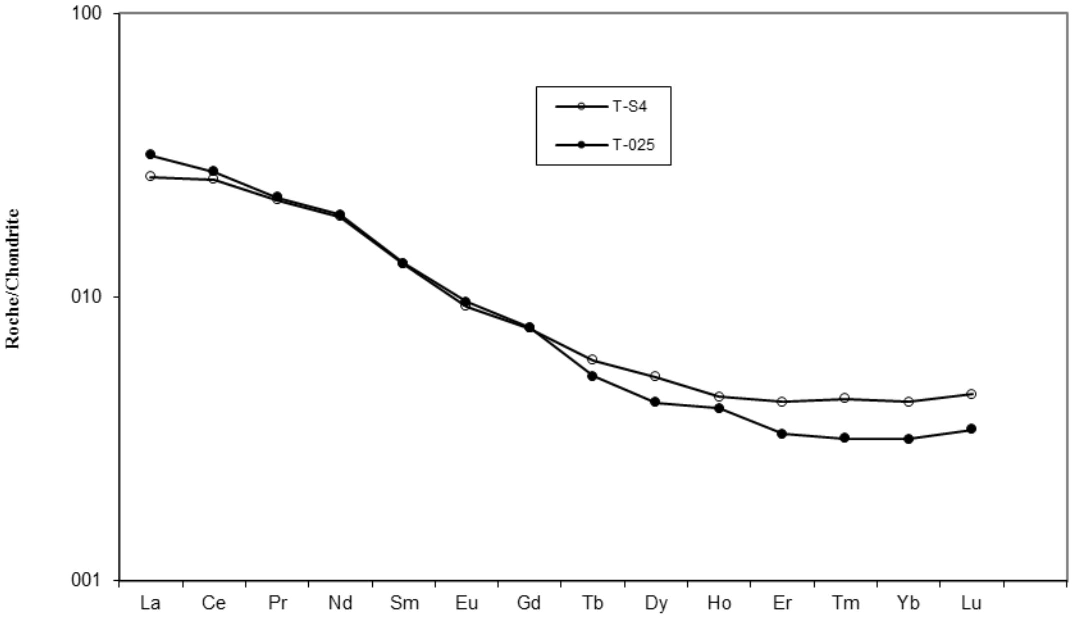

Figure 7 : Selected chondrite normalised REE patterns for Seguela xenoliths cumulates (T025 and TS4) samples [14].

© **Associated Asia Research Foundation (AARF)**
A Monthly Double-Blind Peer Reviewed Refereed Open Access International e-Journal - Included in the International Serial Directories.

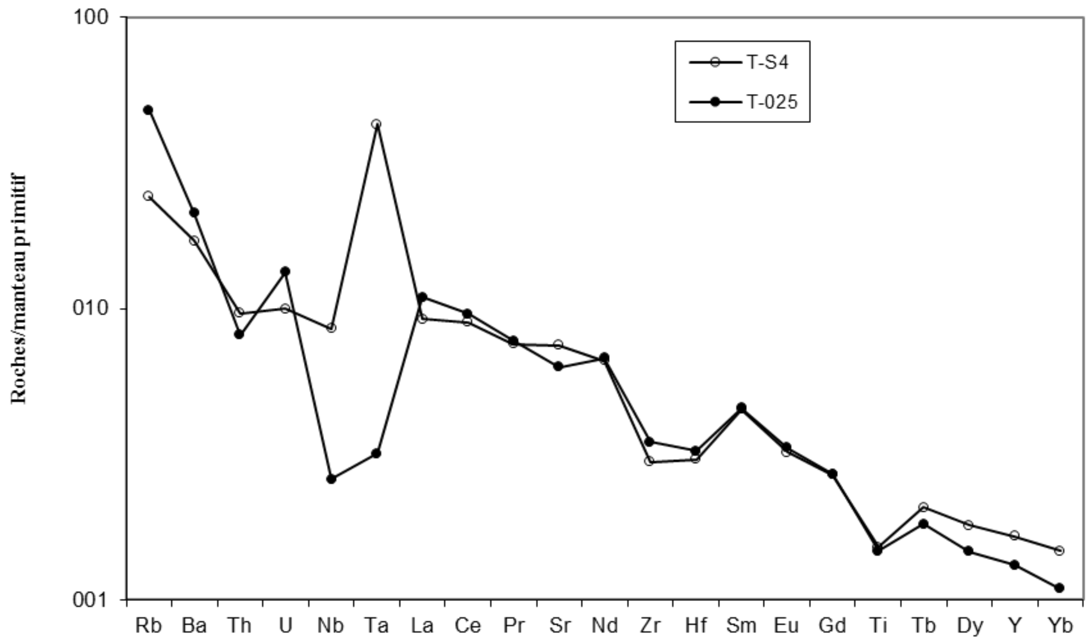

Figure 8 : Average Seguela xenoliths cumulates (T025 and TS4) elements abundance patterns normalized against primitive mantle [14].

5. DISCUSSION

It is noted that the xenoliths cumulate analysis from Seguela has lower values of FeO T, MgO, CaO and Ni, consistent with olivine fractionation from a more primitive melt. An important feature is the presence of the large megacryst suite. The *Mg* values for the three megacrysts phases differ significantly, precluding a simple one-stage model, especially since they show very little compositional variation. The amphibole megacrysts have the lowest Mg values (mostly Mg71, occasionally Mg61*)*, whereas the pyroxene and mica values are closer, but still do not overlap. If the amphibole megacrysts had formed in equilibrium with a parental (peridotitic) silicate melt, it would have to have been more evolved and Fe-rich than the parent melt to the mica and pyroxene megacrysts. The pyroxene is enstatitic with MgsT.83 and the mica has Mg80[10,12,15]. This, together with the euhedral form of these crystals, suggests that the pyroxene megacrysts formed in a melt under ideal fluxing conditions, and not from disaggregation of mega-grained xenoliths. The megacryst pyroxenes differ in having higher TiO_2 values, with lesser amounts of Na_20 and Cr_20_3, compared with the xenolith pyroxenes. The simplest explanation for the megacrysts requires repeated derivation of silicate melts with a range of *Mg* values. Both the mica and amphibole megacrysts could be the remnants of widespread metasomatic veins formed in kimberlites and xenoliths ([3]; [4]; [12]) with a range of *Mg* values. However, their large sizes suggest a pegmatoidal environment, with growth encouraged by volatile fluxing. The micas, in particular, plot very close to phlogopite from the cumulates and kimberlites. It might therefore be supposed that the peridotite micas lie on a series of tie-lines/mixing lines between:

i) the established mantle mica (high Cr, low Ti); and *ii)* the parental melt to the megacrysts (high Ti, low Cr). The spread of Cr contents tends to support this scenario.

The xenoliths have all been metasomatised. Much olivine appears to have been replaced by mica, and both mica and amphibole occur in veins throughout the xenoliths [9]. This metasomatism may have been directly caused by the silicate melt(s) parental to Seguela itself, but it is also likely that the mantle beneath Seguela has been affected by numerous melt generations locally. The alteration of mantle peridotite, in the presence of oxidising fluids, to form olivine pyroxenites is well known ([3, 16]). This appears to have occurred in the mantle under Seguela, and would explain the range of mineralogies seen. The presence of amphibole-mica-olivine cumulates as xenoliths suggests that the melt was arrested long enough for fractionation of olivine to take place, whilst amphibole and/or mica formed the intercumulus phases [17,18,]. The absence of garnet further suggests pressures below about 3.0 GPa. Therefore, those cumulates with both intercumulus phases can probably be restricted to this P-T bracket, corresponding to depths of 60-90 km.

Compared with kimberlites, these olivine pyroxenite xenoliths show high enrichment in HFSE, LILE, REE [2,19]. Their low La/Yb (<14) ratios, and Ba (<150 ppm), Rb (<50 ppm) and Nb (<6 ppm) contents indicate high degree of partial melting. Zr/Hf (39) and Nb/Ta (14) ratios support their lithospheric mantle origin [3, 4, 7, 9, 21]. The age of these olivine pyroxenite xenoliths as derived from zircon is Paleoproterozoic. The geochemical signatures observed on these olivine pyroxenite xenoliths are different from those of continental basalts. This indicate that the arc magmatism in the region derived from ancient subduction process in that affected the composition of the lithospheric mantle modification and lead to the continental tholeiitic arc signatures observed on olivine pyroxenite xenoliths from Côte d’Ivoire [7,8,9,6,13,14,15,20,24,25,26,27].

CONCLUSION

Examination of the xenoliths cumulates reveals a complex multistage igneous history. Numerous generations of melts have metasomatised the lithosphere beneath Seguela, and the kimberlitic pipes and dikes are likely in some way to be related. Previous experimental work has shown that xenoliths cumulates can form by partial melting of metasomatised mantle at -

90 km under conditions of high CO2/H20. The olivine fractionated out of the melt, with mica and/or amphibole forming intercumulus phases probably in the depth range 60-90 km.

The geochemical signatures observed on these olivine pyroxenite xenoliths are different from those of continental basalts. This indicate that the arc magmatism in the region derived from ancient subduction process in that affected the composition of the lithospheric mantle modification and lead to the continental tholeiitic arc signatures observed on olivine pyroxenite xenoliths from Côte d'Ivoire.

ACKNOWLEDGMENTS

This study was supported in part by cooperation between UFRSTRM University of Cocody-Abidjan and University of Orleans. Fields studies to Seguela were supported by SODEMI, and Ivory Coast geology Direction. Assitance for fieldwork was provided by the ministry of Energy and Mines, Ivory Coast. For financial support, sampling privilege and laboratory aid we extend our sincere appreciation. Assistance for laboratory work from CRPG-Nance is acknowledged and MEA acknowledge support from the 9IKC organising committee for financial support.

REFERENCES

[1] Milési, J.P., Feybesse, J.L., Ledru, P., Dommanget, A., Quedraogo, M.F., Marcoux, E., Prost, A., Vinchon., C., Sylvain, J.P., Johan, V., Tegyey, M., Calvez J.Y. and Lagny, P (1989). Les minéralisations aurifères de l'Afrique de l'Ouest. Leurs relations avec l'évolution lithostructurale au Protérozoïque inférieur. Chronique de la Recherche Minière, 497, 3-98

[2] Taylor, W.R., Tompkins, L.A., & Hggerty, S.E., 1994. Comparative geochemistry of West African kimberlites : Evidence for micaceous kimberlites endmember of lithospheric origin. Geochem. Comochem. Acta 58, 4017-4037.

[3] Foley, S. F. 1991. High-pressure stability of the fluorand hydroxy endmembers of pargasite and K-richterite. Geochimica Cosmochimica Acta 55, 2689-2694

[4] Mitchell, R.H., 1995. Kimberlites, orangeites and related rocks. Plenum, New York, 410

[5] Allialy, M.E., Batumike, Jacques. M ; Djro, S.C., Coulibaly, Y., Kouamelan, A.N., Daouda, Y.B., Pouclet., A. (2011b). Chromite, Mg-ilmenite and Priderite as Indicators Minerals of diamondiferous cretaceous Kimberlites and Lamproites from Côte d'Ivoire (West Africa). E.J.S.R. ISSN 1450-216X Vol.48 No.4 (2011), pp.665-693.

[6] Pouclet, A., Allialy, M.E., Yao, D.B., Botty, E., 2004. Découverte d'un diatrème de kimberlite diamantifère à Séguéla en Côte-d'Ivoire. C.R. Géosciences., 336, 9-17.

[7] Allialy, M.E., 2006. Pétrologie et géochimie des kimberlites diamantifères de Séguéla (Centre-Ouest de la Côte d'Ivoire). Thèse de Doctorat. Univ. Abidjan-Cocody, 162 p.
[8] Mitchell, R.H., 1986. Kimberlites Mineralogy, geochemistry, and petrology. Plenum, New York, 442 pp.

[9] Dawson, J. B., Smith, J. V. and Jones, A. P. 1985. A comparative study of bulk rock and mineral chemistry of olivine melilitites and associated rocks from East and South Africa. Neues Jarbuch Mineroligsiche Abhandlungen 152, 143-175.
[10] Foley, S.F., 1991. Higher-pressure stability of fluor and hydroxyendmembers of pargasite and K-richerite. Geochim. Cosmochim. Acta 55, 2689-2694.
[11] Knopf, D., 1970. Kimberlites and related rocks from Côte d'Ivoire. Bull. n. 3, SODEMI, Abidjan, 202 pp.
[12] Foley, S. F. 1992. Vein-plus-wall-rock melting mechanisms in the lithosphere and the origin of potassic alkaline magmas. Lithos 28, 187-204.
[13] Leake, B.E. (1997). Nomenclature of amphiboles. Report of the subcommitee on amphiboles of International Mineralogical Association, Commission on new minerals and new names. Eur. J. Mineral., 9, 623-655.

[14] Sun, S. S. & McDonough, W. F. (1989). Chemical and isotopic systematics of oceanic basalts: implications for mantle composition and processes. Geological Society Special Publication, 42, 313-345.

[15] Konzett, J. 1996. Phase relations and stability of potassium amphiboles in the Earth's mantle: an experimental investigation and a field-based study on MARID-type xenoliths. Ph. D. thesis, E.T.H.,Switzerland.
[16] Brey, G. 1978. The origin of olivine melilitites – chemical and experimental constraints. Journal Volcanology Geothermal Research 3, 61-88.
[17] Lloyd, F.E., Arima, M., Edgar, A.D.,1985. Partial melting of a phlogopite clinopyroxenite nodule from southwest Uganda : an experimental study bearing on the origin of highly potassic continental rift volcanics. Contrib. Mineral. Petrol. 91, 321- 329.
[18] Dawson, J.B., 1980. Kimberlites and their Xenoliths. Spriner-Verlag, New York.
[19] Dawson, J.B., 1971. Advences in kimberlite geology. Earth Sci. Rev. 7, 187-214.
[20] Fieremans, M., Hertogen, J., Demaiffe, D., 1984. Petrology, geochemistry and strontium isotopic composition of the Mbuji-Mayi and Kundelungu kimberlites (RD.Congo). In Kimberlites I: Kimberlites and Related Rocks (ed. J. Kornprobst), pp. 107-120.

© Associated Asia Research Foundation (AARF)

[21] Batumike, J.M., 2008. Origin of kimberlites from Kundelungu Region: Lithospheric Mapping, Diamond potential and crustal Evolution in Southern Democratic Republic of Congo. PhD Thesis, Dept Earth and Planetary Sciences, Macquarie University, 336 pp.
[22] Allialy, M.E., Djro, S.C., Coulibaly, Y., Kouamelan, A.N., Daouda, Y.B., Pouclet., A. 2011a. Comparative geochemistry of Seguela Cretaceous kimberlites, South Africa Group II kimberlites and other worldwide kimberlites. E.J.S.R. ISSN 1450-216X Vol.48 No.3 (2011), pp.665-693.
[23] Graham, S., 1999. The petrogenisis of alkaline ultramafic and related rocks from eastern Yilgran craton, Western Australia. PhD Thesis, Monash University, 285p.
[24] Graham, S., Lambert, D.D., Shee, S.R., Pearson, N.J., 2002. Juvenile Lithospheric mantle enrichment and the formation of alkaline ultramafic magma sources: Re-Os, Lu-Hf and Sm-Nd isotopic systematics of the Norseman melnoites, Western Australia. Chemical Geology, 186, 215-233.
[25] Weaver B.L., Wood, D.A., Taraney, J., Joron, J.L., 1987. Geochemistry of ocean island basalt from the south Atlantic: Ascesion Bouvet, St. Helena, Gough and Tristan da Cunha. In: Fitton, J.G., Upton, G.J. (Eds), Alkaline Igneous Rocks, Geol. Soc. London, 253-267.

[26] Rogers, N.W., Hawkesworth, C.J., Palacs, Z.A., 1992. Phlogopite in the generation of olivine-melilitites from Namaqualand, South Africa and implication for element fractionation processes in the upper mantle. Lithos 28, 347- 365.
[27] Hawkesworth, C.J., Mantovani, M.S., Tayor, P.N., Palacz, Z., 1986. Evidence from the Parana of south Brazil for a continental contribution to Dupal basalts. Nature, 356-359.